Asymmetric excitations of toroidal dipole resonance and the magnetic dipole quasi-bound state in the continuum in an all-dielectric metasurface

LI, Bin; YAO, Jin; ZHU, Han; CAI, Guoxiong; LIU, Qing Huo

Published in:
Optical Materials Express

Published: 01/07/2021

Document Version:
Final Published version, also known as Publisher's PDF, Publisher's Final version or Version of Record

Published version (DOI):
10.1364/OME.430723

Publication details:
LI, B., YAO, J., ZHU, H., CAI, G., & LIU, Q. H. (2021). Asymmetric excitations of toroidal dipole resonance and the magnetic dipole quasi-bound state in the continuum in an all-dielectric metasurface. *Optical Materials Express*, *11*(7), 2359-2368. https://doi.org/10.1364/OME.430723

Research Article | Vol. 11, No. 7 / 1 July 2021 / Optical Materials Express 2359
Optical Materials EXPRESS

Asymmetric excitations of toroidal dipole resonance and the magnetic dipole quasi-bound state in the continuum in an all-dielectric metasurface

Bin Li,[1,3] Jin Yao,[1,3] Han Zhu,[1] Guoxiong Cai,[1,*] and Qing Huo Liu[2]

[1]Institute of Electromagnetics and Acoustics, and Fujian Provincial Key Laboratory of Electromagnetic Wave Science and Detection Technology, Xiamen University, Xiamen 361005, China
[2]Department of Electrical and Computer Engineering, Duke University, Durham, North Carolina 27708, USA
[3]These authors contributed equally to this work
[*]gxcai8303@xmu.edu.cn

Abstract: All-dielectric resonant metasurfaces are expected to boost Mie resonances with high Q-factors and enhanced electromagnetic fields owing to their large mode volumes and low material losses. However, the toroidal dipole (TD) and magnetic dipole (MD) are usually suppressed by other stronger multipoles due to their relatively weak coupling to the incident lights. In this work, the double resonances of TD and MD quasi-bound state in the continuum (quasi-BIC) are excited asymmetrically by breaking the geometric symmetry in an all-dielectric metasurface consisting of arrays of silicon I-bars and silicon Φ-disks, leading to their corresponding enhanced electric field confinements and high Q-factors. The sensing performances by these two resonances are investigated as well, achieving refractive index sensitivities of 784.8 nm/RIU and 630 nm/RIU, respectively. This work suggests a route to manipulate strong TD and MD quasi-BIC excitations and facilitates their practical applications such as nonlinear light sources and sensing.

1. Introduction

Metasurfaces, as 2D forms of metamaterials, have extraordinary resonant optical responses and have been extensively employed in nanophotonics [1,2]. The surface plasmon resonances can be excited by sub-wavelength metallic metasurfaces, while their Q-factors are limited on account of high inherent resistive losses in the metals [3]. Therefore, all-dielectric metasurfaces with small dissipation and high laser damage threshold have been proposed, which can support Mie resonances with high Q-factors and low absorption losses [4]. They possess great capabilities of confining and enhancing the near field inside the nanoparticles, which govern the performance of many applications, such as harmonic generation [5,6], Raman scattering [7], and sensing [8,9].

Toroidal dipole (TD) is one of the members of Mie multipoles in all-dielectric metasurfaces, which originates from two inverse circulating currents [10–12]. Compared with electric dipole (ED) and magnetic dipole (MD), TD has weaker capabilities of confining and enhancing the near field [13,14]. Many researches about enhancing TD response have been reported. By manipulating the near-field coupling and the geometry arrangement, the strong and nearly pure TD resonance can be achieved in all-dielectric metasurfaces composed of clusters of subwavelength high-index dielectric cylinders [15,16]. Regulating the asymmetric permittivities of the components in all-dielectric metasurfaces is also an effective way to excite and boost the TD response [17], providing an efficient platform for sensing and optical nonlinearity. However, the electric field enhancements and Q-factors of TD resonances in the existing work are still

#430723 https://doi.org/10.1364/OME.430723
Journal © 2021 Received 6 May 2021; revised 13 Jun 2021; accepted 19 Jun 2021; published 28 Jun 2021

Optical Materials EXPRESS

insufficient, which require further explorations in structure design and physical mechanism innovation.

Bound state in the continuum (BIC) can produce extremely high Q resonances, which appears firstly in quantum mechanics, and then is reported in other fields such as optics, acoustics, hydrodynamics, and etc. [18–22]. A true BIC only appears in ideal lossless infinite structures or extreme values of parameters, and its resonance linewidth disappears while its Q-factor is infinite [23–25]. Normally, the BIC is symmetrically protected since the coupling constants vanish accidentally due to symmetry [26]. Recently it is revealed that symmetry-protected BIC can be transformed into quasi-BIC with a finite yet sharply high Q resonance by breaking the symmetry [27–29]. Some structures supporting quasi-BIC have also been reported, such as nanoholes [30,31], circular slots [32], and etc, implying outstanding performances in various applications, such as high Q cavity-mode laser [33], dynamical image tuning and display [34], and enhancing the nonlinear interactions between light and matter [35].

In this work, we propose the asymmetric excitations of TD resonance and MD quasi-BIC in an I-Φ shaped all-dielectric metasurface related to the parameter of distance difference. First, double resonances with giant enhancements of electromagnetic fields and extremely high Q-factors are excited. Then, by adjusting the distance difference between the I-bar and the neighboring Φ-disks, the physical mechanisms of double resonances are demonstrated. Finally, the sensing performances by these two resonances are investigated as well.

2. Structure design and double resonances properties

The proposed all-dielectric metasurface has a square-lattice pattern, as shown in Fig. 1, whose unit cell consists of a silicon I-shaped bar and a silicon Φ-shaped disk surrounded by air. The dispersive refractive indexes of silicon are taken from its experimentally measured data [36]. A y-polarized plane wave propagating along the z-axis is illuminated normally upon the metasurface. The numerical optical responses of the proposed silicon I-Φ shaped metasurface are simulated by commercial software COMSOL Multiphysics^{TM} based on the finite element method. Periodic boundary conditions are applied in the x- and y-directions, while perfectly matched layers are

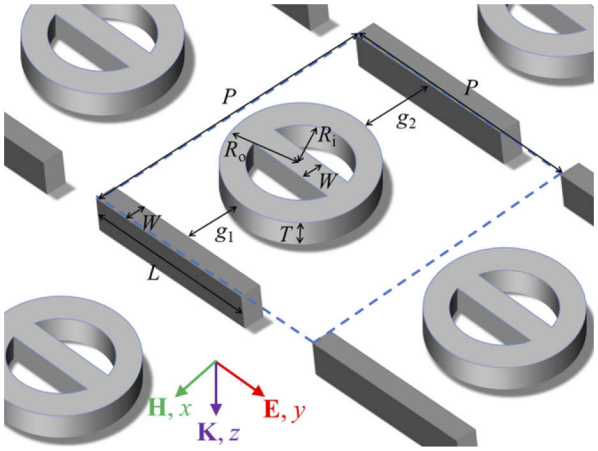

Fig. 1. Schematic illustration of the proposed silicon I-Φ shaped metasurface consisting of I-bars and Φ-disks. Geometric parameters: length of I-bars $L = 790$ nm, width and thickness of nanorods for both I-bars and Φ-disks $W = 60$ nm and $T = 120$ nm, inner and outer radius of Φ-disks $R_i = 240$ nm and $R_o = 300$ nm, and period of the metasurface $P = 1000$ nm. Distance difference $\Delta g = g_2 - g_1$.

Optical Materials EXPRESS

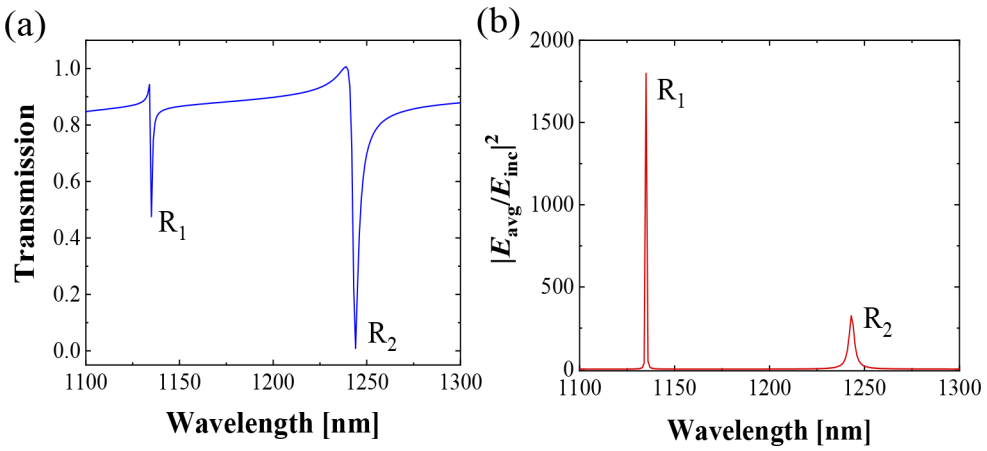

Fig. 2. Spectra as functions of wavelength. (a) Transmission, and (b) average enhancement factor $|E_{avg}/E_{inc}|^2$.

used to truncate the infinite space along the z-direction. The practical fabrication can be readily operated on silicon film by electron-beam lithography and reactive-ion etching techniques [37,38].

As is well known, the bar-disk tandem structures have been proposed to support Fano resonances [37–5]. However, the excitations of the TD and MD resonances were usually difficult due to their relatively weak coupling to the incident lights. The design consideration of the proposed metasurface lies on the overlap between the anapole and the electric dipole (ED) resonances. The Φ-disk array supports structured anapole modes [39], while the I-bar array excites ED modes. When the geometric parameters are chosen carefully to let them overlap at a same wavelength of 1072 nm (spectrum not shown for simplicity), and the array is arranged by both of the I-bar and Φ-disk, the structured MD dark modes in the Φ-disks would be induced and suppress the structured anapole modes. This is because the dipole axis of the structured MD modes is out-of-plane, and it is easy to be excited by the magnetic field of a co-plane ED mode rather than that of the normally incident wave, which appears to be perpendicular to the axis [37].

To start with, we define $\Delta g = g_2 - g_1$ as the distance difference between the bar and the neighboring disks. As $\Delta g \neq 0$, the symmetry of the structure will be broken. Figure 2(a) gives the transmission spectrum of the proposed metasurface for $\Delta g = 200$ nm. It can be seen that two prominently sharp dips, Resonance R_1 and Resonance R_2, appear on the almost transparent spectrum in the wavelength range of 1100 nm ~ 1300 nm, indicating the double resonances are excited. The widths of both resonances are narrow, implying the high Q-factors and the strong electromagnetic field confinement. Indeed, one of the fascinating properties of the all-dielectric metasurface is its ability to confine the electric field inside the dielectric nanostructures, which facilitates the practical applications of nonlinear frequency conversion, nanolaser, and etc. Therefore, the average electric field enhancement factor is introduced to quantify the normalized electric field intensity averaged within the silicon nanostructure [40], which is expressed as followed

$$|E_{avg}/E_{inc}|^2 = \frac{\iiint |E|^2 dV}{|E_{inc}|^2 V} \tag{1}$$

where $|E|$ is the local electric field inside the silicon nanostructures, $|E_{inc}|$ is the amplitude of the incident electric field, and V the volume of the silicon nanostructures. Figure 2(b) presents the average enhancement factor as functions of the wavelength. It can be seen that two typical Lorentz line shapes emerge, corresponding to the two Fano-like resonances in Fig. 2(a). In the following, we will investigate the asymmetric excitations of the double resonances by the average

Optical Materials EXPRESS

enhancement factors at the resonant wavelengths and their corresponding Q-factors, which are extracted from the Lorentz line shapes rather than the Fano-like line shapes in the transmission spectrum in Fig. 2(a).

3. Results and discussions

3.1. Dependence on distance difference Δg

Figure 3(a) demonstrates the dependence of the transmission spectra on the distance difference Δg. It can be seen that the double resonances are symmetric with respect to $\Delta g = 0$. However, the excitations of these two resonances are asymmetric. With the decreasing of $|\Delta g|$, Resonance R_1 has a red shift and the line width is broadened, while Resonance R_2 has a blue shift and the line width is narrowed. Moreover, it is interesting that R_2 disappears at $\Delta g = 0$, as indicated by the white dash circle. For both resonances, their Fano-like line shapes might vary dramatically, but their abilities to confine electromagnetic can be directly manifested on the spectra of average enhancement factor. We thus calculate the spectra of average enhancement factors and extract their corresponding properties.

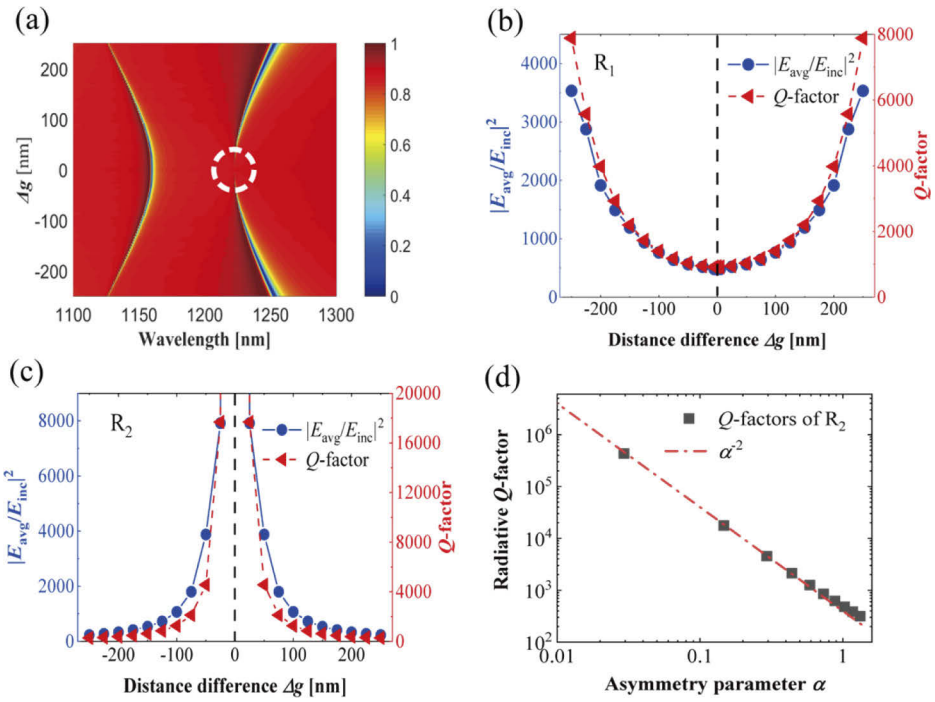

Fig. 3. (a) Transmission spectra of the proposed metasurface as functions of wavelength and distance difference Δg. (b) and (c), dependences of average enhancement factor and Q-factor on Δg of Resonances R_1 and R_2, respectively. (d) Relationship between the Q-factor of R_2 and the asymmetry parameter α.

First of all, the average enhancement factor extracted at the resonant wavelength of Resonance R_1 and its corresponding Q-factor as the functions of Δg are given in Fig. 3(b). It can be seen that as $|\Delta g|$ enlarges, the average enhancement factor is increased. The corresponding Q-factor is increased synchronously, indicating that the electric field localization comes inherently from the mode resonance. As $|\Delta g|$ reaches 250 nm, the average enhancement factor and the Q-factor are as high as 3533 and 7885, which are 7 folds and 9 folds when compared to those of $|\Delta g| = 0$,

Optical Materials EXPRESS

respectively. Secondly, in contrast to R_1, R_2 experiences a totally different excitation, as shown in Fig. 3(c). The average enhancement factor and the Q-factor both grow exponentially and approach infinity as $|\Delta g|$ decreases. As $|\Delta g|$ reaches 25 nm, they are as high as 7917 and 17684, which are 34 folds and 62 folds when compared to those of $|\Delta g| = 250$ nm, respectively. These extremely high average enhancement factor and Q-factor indicate the great potentials of the proposed all-dielectric metasurface in the applications of nonlinear optics and nanolaser [41,42].

Mathematically, a true bound state in the continuum (BIC) has infinite value of the Q-factor, but it is in fact a "dark mode", which does not manifest itself in the R_2 transmission spectrum in Fig. 3(a). However, the average enhancement factor and Q-factor of R_2 are not infinite but disappear suddenly as $|\Delta g|$ decreases to be 0, and this can be regarded as the symmetry-protected BIC. Interestingly, the symmetry-protected BIC is easily destroyed by breaking the geometric symmetry to induce leakage, generating the quasi-BIC with radiative loss when $|\Delta g| > 0$ [43]. To further verify this judgment, we fit the relationship between the Q-factor of R_2 and the asymmetry parameter α, as shown in Fig. 3(d). α is defined as $\Delta g/g$, and g is the distance between the I-bars and the Φ-disks at $\Delta g = 0$. It can be seen that the evolution of the Q-factor of R_2 is consistent with the theoretical formula between the radiative Q-factor Q_{rad} and the α [26],

$$Q_{rad} \propto \alpha^{-2}. \tag{2}$$

The perfect match with the inverse quadratic law of Eq. (2) indicates that R_2 can be recognized as a quasi-BIC, which is featured to have an extremely high Q-factor as α approaching zero.

In order to analyze the physical origins of these two resonances, the Cartesian multipole decompositions [44] are performed and those for the distance difference $\Delta g = 0$, 25 nm, 100 nm and 200 nm are presented in Fig. 4. For Resonance R_1, although there are some other dipoles mixing in, the toroidal dipole (TD) contributes more. As Δg increases, the intensities of these dipoles change, but TD always dominates, and its line width is getting narrower. Hence, R_1 can be theoretically attributed to be the TD. On the other hand, for R_2, it is a pure MD resonance when $\Delta g = 0$. However, it is really weak and submerges on the flat curve of other dipole moments, as shown in Fig. 4(a). As the symmetry breaks and Δg increases to be 25 nm, this symmetry-protected BIC is transformed into the quasi-BIC, and the MD floats up and surpasses all other moments, as shown in Fig. 4(b). As Δg increases further, there are some other dipoles mixing in, and the line width of MD is getting wider. Nevertheless, the MD is the dominated dipole of R_2, and its evolution corresponds to the Q-factors in Fig. 3(c).

To further verify the origins of these two resonances, Fig. 5 demonstrates the corresponding electromagnetic field distributions. For Resonance R_1 in Fig. 5(a), when $\Delta g = 0$, there has two opposite circular currents, revealing the pattern of TD. However, these two currents evenly distribute on two sides of Φ-disk, which can be considered to be two MDs in opposite directions. Therefore, the destructive interference of these two opposite MDs leads to the weakest ability of confinement. When $|\Delta g| > 0$, as mentioned above, more dipoles are mixed in, and one of the circular currents is destroyed, leaving the other one. As Δg increases, the only existing circular current approaches to the center of Φ-disk, resulting in that the electric field is enhanced inside the dielectric structures, which corresponds to the dependence of average enhancement factor and Q-factor on Δg in Fig. 3(b). On the other hand, for the MD quasi-BIC of R_2 in Fig. 5(b), when $\Delta g = 0$, the distributions of both electric and magnetic fields have no any feature. However, as Δg slightly increases to be 25 nm, the quasi-BIC is formed and the circular current of MD emerges around the center of Φ-disk, leading to the extremely high localization and enhancement of electric field inside the dielectric structures of Φ-disk. As Δg increases further, the circular current moves away from the center of Φ-disk, leading to the rapidly degradation of the electromagnetic field. Together with the evolution in Fig. 5(a), it is exactly the position of circular current with respect to the center of Φ-disk leading to the asymmetric excitations of R_2 and R_1, which have been demonstrated in Fig. 3(a)-(c).

Optical Materials EXPRESS

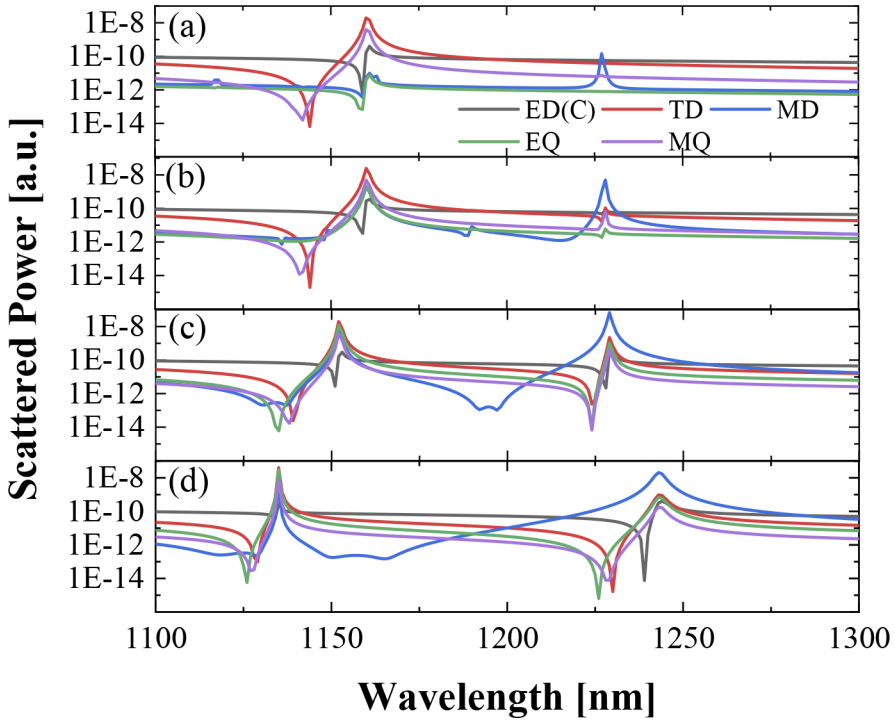

Fig. 4. Cartesian multipole decompositions of the two resonances (R_1 on the left, while R_2 right) for (a) $\Delta g = 0$, (b) $\Delta g = 25$ nm, (c) $\Delta g = 100$ nm, and (d) $\Delta g = 200$ nm. ED(C), TD, MD, EQ, and MQ represent the Cartesian electric dipole, toroidal dipole, magnetic dipole, electric quadrupole and magnetic quadrupole, respectively.

3.2. Refractive index sensing

Besides the ability to confine the electric field inside the dielectric nanostructure, the proposed metasurface also has the opportunity to be applied in refractive index (RI) sensing. In practical operations, the loss and the surface roughness of the metasurfaces will influence the resonances thus the sensing performance. Here, they are not considered for simplicity. Figures 6(a) and (b) give the resonant wavelength shifts as the function of the RI for Resonances R_1 and R_2, respectively. The sensing analyte is set as the infinite surrounding medium. It is interesting to be seen that the wavelength shifts of both resonances are proportional to the variation of RI no matter how Δg changes. This stems from the fact that the electric field energies of high Q resonances are mainly confined inside the dielectric nanostructure, and rarely distributed in the surrounding medium. Therefore, the RI sensing capabilities depend more on the modes themselves rather than on the electric field hot spot on the surrounding sensing medium [45,46].

Nevertheless, the structured modes supported by the proposed metasurface have high sensing abilities. The refractive index sensitivities (RISs) are as high as 784.8 nm/RIU and 630 nm/RIU for R_1 and R_2, respectively, and they are almost independent on the distance difference Δg. The zero wavelength shift for R_2 under $\Delta g = 0$ is because there is no resonant mode formed due to the symmetry-protected BIC. The RISs based on all-dielectric metasurfaces have been previously explored in Table 1. Compared with these published works, the proposed metasurface has higher RISs. Together with the ease of fabrication resulting from the independence on Δg, the modes supported by our proposed metasurface have great potential for RI sensing application.

Optical Materials EXPRESS

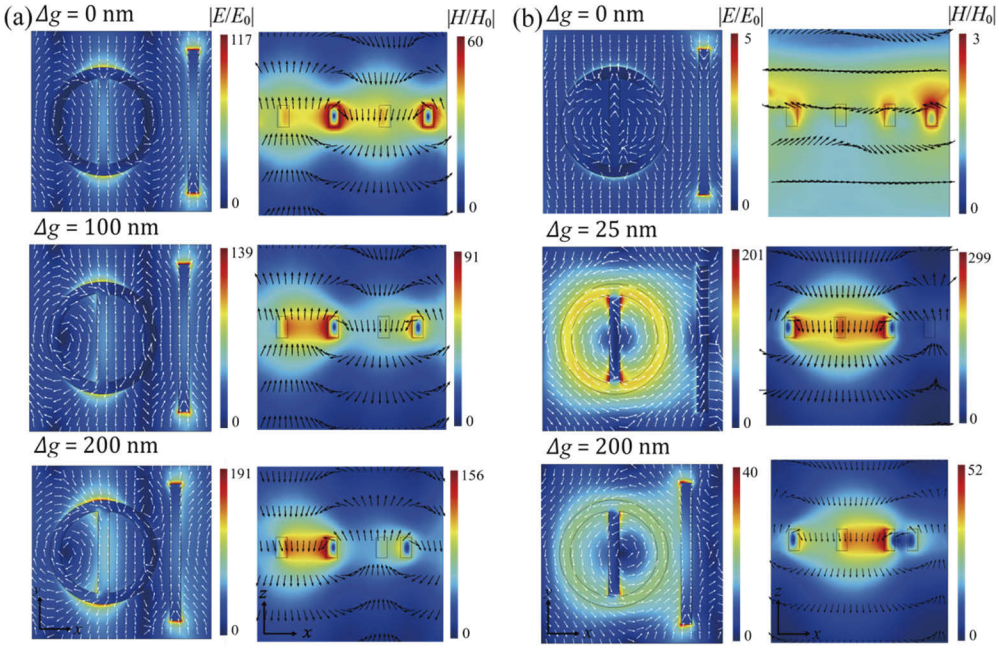

Fig. 5. Normalized electric fields distributions $|E/E_0|$ on the *xy*-plane and normalized magnetic fields distributions $|H/H_0|$ on the *xz*-plane for different values of Δg. The electric field vectors (white arrows) and magnetic field vectors (black arrows) are also presented in their corresponding patterns, (a) R_1 and (b) R_2.

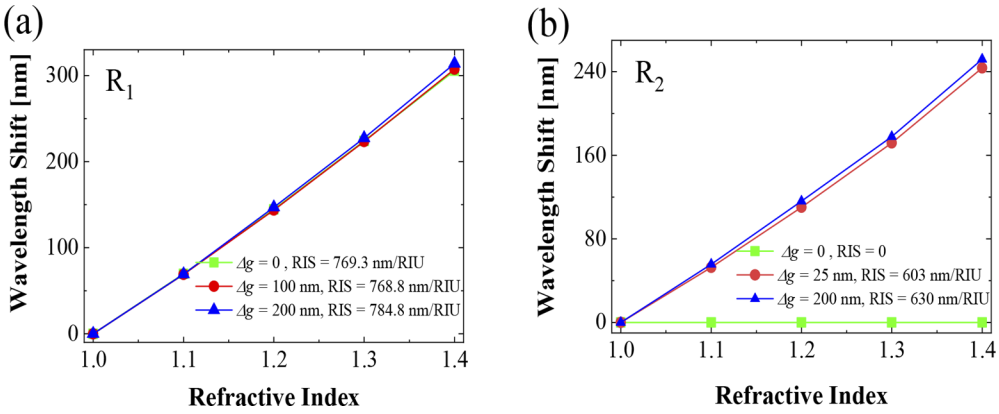

Fig. 6. Dependences of resonant wavelength shift on refractive index of surrounding medium, (a) R_1 and (b) R_2.

Table 1. Comparison of the sensitivity of similar works published previously[a]

Structure	Type of metasurface	Sensitivity (nm/RIU)
Bar-disks [37]	EIT resonance	289
Asymmetric paired bars [47]	Multiple Fano resonances	370
Dielectric gratings [48]	BIC resonance	252.3
Asymmetrical cylinders [49]	Fano resonance	541
This work	TD and MD quasi-BIC resonances	784.8

[a]EIT: electromagnetically induced transparency

Optical Materials EXPRESS

4. Conclusion

In summary, we have demonstrated that by breaking the geometric symmetry in an all-dielectric metasurface consisting of arrays of silicon I-bars and silicon Φ-disks, TD resonance and MD quasi-BIC are excited asymmetrically by the distance difference Δg, realizing giant enhancements of electromagnetic fields and extremely high Q-factors. Numerical results show that the average enhancement factor and the Q-factor of TD resonance are as high as 3533 and 7885 when $\Delta g = 250$ nm, and those of MD resonance governed by quasi-BIC can be as high as 7917 and 17684 when $\Delta g = 25$ nm. Furthermore, the sensing performances by these two resonances are investigated as well, achieving refractive index sensitivities of 784.8 nm/RIU and 630 nm/RIU, respectively, which are higher than those of previous works based on all-dielectric metasurfaces. Our proposed all-dielectric metasurface broadens the way to efficiently tailor strong TD and MD quasi-BIC excitations, and provides promising prospects for applications in light sources, sensing and many other aspects.

Funding. National Natural Science Foundation of China (11604276, 61871462); National Key Research and Development Program of China (2018YFC0603503).

Disclosures. The authors declare no conflicts of interest.

Data availability. Data underlying the results presented in this paper are not publicly available at this time but may be obtained from the authors upon reasonable request.

References

1. A. E. Minovich, A. E. Miroshnichenko, A. Y. Bykov, T. V. Murzina, D. N. Neshev, and Y. S. Kivshar, "Functional and nonlinear optical metasurfaces," Laser Photonics Rev. **9**(2), 195–213 (2015).
2. H. T. Chen, A. J. Taylor, and N. Yu, "A review of metasurfaces: physics and applications," Rep. Prog. Phys. **79**(7), 076401 (2016).
3. M. Allione, V. V. Temnov, Y. Fedutik, U. Woggon, and M. V. Artemyev, "Surface plasmon mediated interference phenomena in low-Q silver nanowire cavities," Nano Lett. **8**(1), 31–35 (2008).
4. Q. Zhao, J. Zhou, F. Zhang, and D. Lippens, "Mie resonance-based dielectric metamaterials," Mater. Today **12**(12), 60–69 (2009).
5. H. Liu, C. Guo, G. Vampa, J. L. Zhang, T. Sarmiento, M. Xiao, P. H. Bucksbaum, J. Vučković, S. Fan, and D. A. Reis, "Enhanced high-harmonic generation from an all-dielectric metasurface," Nat. Phys. **14**(10), 1006–1010 (2018).
6. W. Tong, C. Gong, X. Liu, S. Yuan, Q. Huang, J. Xia, and Y. Wang, "Enhanced third harmonic generation in a silicon metasurface using trapped mode," Opt. Express **24**(17), 19661–19670 (2016).
7. S. Romano, G. Zito, S. Managò, G. Calafiore, E. Penzo, S. Cabrini, A. C. De Luca, and V. Mocella, "Surface-enhanced Raman and fluorescence spectroscopy with an all-dielectric metasurface," J. Phys. Chem. C **122**(34), 19738–19745 (2018).
8. J. Zhang, W. Liu, Z. Zhu, X. Yuan, and S. Qin, "Strong field enhancement and light-matter interactions with all-dielectric metamaterials based on split bar resonators," Opt. Express **22**(25), 30889–30898 (2014).
9. T. Ma, Q. Huang, H. He, Y. Zhao, X. Lin, and Y. Lu, "All-dielectric metamaterial analogue of electromagnetically induced transparency and its sensing application in terahertz range," Opt. Express **27**(12), 16624–16634 (2019).
10. A. Sayanskiy, M. Danaeifar, P. Kapitanova, and A. E. Miroshnichenko, "All-dielectric metalattice with enhanced toroidal dipole response," Adv. Opt. Mater. **6**(19), 1800302 (2018).
11. I. V. Stenishchev and A. A. Basharin, "Toroidal response in all-dielectric metamaterials based on water," Sci. Rep. **7**(1), 9468 (2017).
12. T. Kaelberer, V. A. Fedotov, N. Papasimakis, D. P. Tsai, and N. I. Zheludev, "Toroidal dipolar response in a metamaterial," Science **330**(6010), 1510–1512 (2010).
13. A. B. Evlyukhin, C. Reinhardt, A. Seidel, B. S. Luk'yanchuk, and B. N. Chichkov, "Optical response features of Si-nanoparticle arrays," Phys. Rev. B **82**(4), 045404 (2010).
14. A. I. Kuznetsov, A. E. Miroshnichenko, M. L. Brongersma, Y. S. Kivshar, and B. Luk'yanchuk, "Optically resonant dielectric nanostructures," Science 354(6314), aag2472 (2016).
15. A. A. Basharin, M. Kafesaki, E. N. Economou, C. M. Soukoulis, V. A. Fedotov, V. Savinov, and N. I. Zheludev, "Dielectric metamaterials with toroidal dipolar response," Phys. Rev. X **5**(1), 011036 (2015).
16. V. R. Tuz, V. V. Khardikov, and Y. S. Kivshar, "All-dielectric resonant metasurfaces with a strong toroidal response," ACS Photonics **5**(5), 1871–1876 (2018).
17. X. Liu, J. Li, Q. Zhang, and Y. Wang, "Dual-toroidal dipole excitation on permittivity-asymmetric dielectric metasurfaces," Opt. Lett. **45**(10), 2826–2829 (2020).
18. H. Friedrich and D. Wintgen, "Interfering resonances and bound states in the continuum," Phys. Rev. A **32**(6), 3231–3242 (1985).

Optical Materials EXPRESS

19. R. Parker, "Resonance effects in wake shedding from parallel plates: some experimental observations," Journal of Sound and Vibration **4**(1), 62–72 (1966).
20. F. Ursell, "Trapping modes in the theory of surface waves," Math. Proc. Cambridge Philos. Soc. **47**(2), 347–358 (1951).
21. D. Marinica, A. Borisov, and S. Shabanov, "Bound states in the continuum in photonics," Phys. Rev. Lett. **100**(18), 183902 (2008).
22. E. N. Bulgakov and A. F. Sadreev, "Bound states in the continuum in photonic waveguides inspired by defects," Phys. Rev. B **78**(7), 075105 (2008).
23. R. F. Ndangali and S. V. Shabanov, "Electromagnetic bound states in the radiation continuum for periodic double arrays of subwavelength dielectric cylinders," J. Math. Phys. **51**(10), 102901 (2010).
24. C. W. Hsu, B. Zhen, J. Lee, S. -L. Chua, S. G. Johnson, J. D. Joannopoulos, and M. Soljačić, "Observation of trapped light within the radiation continuum," Nature **499**(7457), 188–191 (2013).
25. C. W. Hsu, B. Zhen, A. D. Stone, J. D. Joannopoulos, and M. Soljačić, "Bound states in the continuum," Nat. Rev. Mater. **1**(9), 16048 (2016).
26. K. Koshelev, S. Lepeshov, M. Liu, A. Bogdanov, and Y. Kivshar, "Asymmetric metasurfaces with high-Q resonances governed by bound states in the continuum," Phys. Rev. Lett. **121**(19), 193903 (2018).
27. Z. F. Sadrieva, I. S. Sinev, K. L. Koshelev, A. Samusev, I. V. Iorsh, O. Takayama, R. Malureanu, A. A. Bogdanov, and A. V. Lavrinenko, "Transition from optical bound states in the continuum to leaky resonances: Role of substrate and roughness," ACS Photonics **4**(4), 723–727 (2017).
28. M. A. Belyakov, M. A. Balezin, Z. F. Sadrieva, P. V. Kapitanova, E. A. Nenasheva, A. F. Sadreev, and A. A. Bogdanov, "Experimental observation of symmetry protected bound state in the continuum in a chain of dielectric disks," Phys. Rev. A **99**(5), 053804 (2019).
29. S. Li, C. Zhou, T. Liu, and S. Xiao, "Symmetry-protected bound states in the continuum supported by all-dielectric metasurfaces," Phys. Rev. A **100**(6), 063803 (2019).
30. S. Xie, C. Xie, S. Xie, J. Zhan, Z. Li, Q. Liu, and G. Tian, "Bound states in the continuum in double-hole array perforated in a layer of photonic crystal slab," Appl. Phys. Express **12**(12), 125002 (2019).
31. S. Xie, S. Xie, J. Zhan, C. Xie, G. Tian, Z. Li, and Q. Liu, "Bound states in the continuum in a T-shape nanohole array perforated in a photonic crystal slab," Plasmonics **15**(5), 1261–1271 (2020).
32. J. Algorri, F. Dell'Olio, P. Roldán-Varona, L. Rodríguez-Cobo, J. López-Higuera, J. Sánchez-Pena, and D. Zografopoulos, "Strongly resonant silicon slot metasurfaces with symmetry-protected bound states in the continuum," Opt. Express **29**(7), 10374–10385 (2021).
33. A. Kodigala, T. Lepetit, Q. Gu, B. Bahari, Y. Fainman, and B. Kanté, "Lasing action from photonic bound states in continuum," Nature **541**(7636), 196–199 (2017).
34. L. Xu, K. Zangeneh Kamali, L. Huang, M. Rahmani, A. Smirnov, R. Camacho-Morales, Y. Ma, G. Zhang, M. Woolley, and D. Neshev, "Dynamic nonlinear image tuning through magnetic dipole quasi-BIC ultrathin resonators," Adv. Sci. **6**(15), 1802119 (2019).
35. K. Koshelev, Y. Tang, K. Li, D.-Y. Choi, G. Li, and Y. Kivshar, "Nonlinear metasurfaces governed by bound states in the continuum," ACS Photonics **6**(7), 1639–1644 (2019).
36. M. R. Shcherbakov, P. Vabishchevich, A. Shorokhov, K. E. Chong, D. Y. Choi, I. Staude, A. E. Miroshnichenko, D. N. Neshev, A. A. Fedyanin, and Y. S. Kivshar, "Ultrafast all-optical switching with magnetic resonances in nonlinear dielectric nanostructures," Nano Lett. **15**(10), 6985–6990 (2015).
37. Y. Yang, I. I. Kravchenko, D. P. Briggs, and J. Valentine, "All-dielectric metasurface analogue of electromagnetically induced transparency," Nat. Commun. **5**(1), 5753 (2014).
38. Y. Yang, W. Wang, A. Boulesbaa, I. I. Kravchenko, D. P. Briggs, A. Puretzky, D. Geohegan, and J. Valentine, "Nonlinear Fano-resonant dielectric metasurfaces," Nano Lett. **15**(11), 7388–7393 (2015).
39. W. Wang, X. Zhao, L. Xiong, L. Zheng, Y. Shi, Y. Liu, and J. Qi, "Broken symmetry theta-shaped dielectric arrays for a high Q-factor Fano resonance with anapole excitation and magnetic field tunability," OSA Continuum **2**(2), 507–517 (2019).
40. J. Yao, Y. Wu, J. Liu, N. Liu, and Q. H. Liu, "Enhanced optical bistability by coupling effects in magnetic metamaterials," J. Lightwave Technol. **37**(23), 5814–5820 (2019).
41. Y. Gao, Y. Fan, Y. Wang, W. Yang, Q. Song, and S. Xiao, "Nonlinear holographic all-dielectric metasurfaces," Nano Lett. **18**(12), 8054–8061 (2018).
42. W. Bi, X. Zhang, M. Yan, L. Zhao, T. Ning, and Y. Huo, "Low-threshold and controllable nanolaser based on quasi-BIC supported by an all-dielectric eccentric nanoring structure," Opt. Express **29**(8), 12634–12643 (2021).
43. Z. Liu, Y. Xu, Y. Lin, J. Xiang, T. Feng, Q. Cao, J. Li, S. Lan, and J. Liu, "High-Q quasi-bound states in the continuum for nonlinear metasurfaces," Phys. Rev. Lett. **123**(25), 253901 (2019).
44. P. C. Wu, C. Y. Liao, V. Savinov, T. L. Chung, W. T. Chen, Y.-W. Huang, P. R. Wu, Y.-H. Chen, A.-Q. Liu, and N. I. Zheludev, "Optical anapole metamaterial," ACS Nano **12**(2), 1920–1927 (2018).
45. N. Liu, M. Mesch, T. Weiss, M. Hentschel, and H. Giessen, "Infrared perfect absorber and its application as plasmonic sensor," Nano Lett. **10**(7), 2342–2348 (2010).
46. G. Cai, W. Li, Y. Chen, N. Liu, Z. Song, and Q. H. Liu, "Modeling and design of a plasmonic sensor for high sensing performance and clear registration," IEEE Photon. J. **8**(1), 4801011 (2016).

Optical Materials EXPRESS

47. Y. Zhang, W. Liu, Z. Li, Z. Li, H. Cheng, S. Chen, and J. Tian, "High-quality-factor multiple Fano resonances for refractive index sensing," Opt. Lett. **43**(8), 1842–1845 (2018).
48. D. N. Maksimov, V. S. Gerasimov, S. Romano, and S. P. Polyutov, "Refractive index sensing with optical bound states in the continuum," Opt. Express **28**(26), 38907–38916 (2020).
49. W. Su, Y. Ding, Y. Luo, and Y. Liu, "A high figure of merit refractive index sensor based on Fano resonance in all-dielectric metasurface," Results Phys. **16**, 102833 (2020).